

# Fabrication of optical filters based on polymer asymmetric Bragg couplers

Wei-Ching Chuang<sup>1</sup>, An-Chen Lee<sup>2,3</sup>, Ching-Kong Chao<sup>4</sup>, and Chi-Ting Ho<sup>2</sup>

<sup>1</sup>*Department of Electro-Optics Engineering*

<sup>2</sup>*Department of Mechanical Design Engineering  
National Formosa University, Huwei, Yulin, Taiwan*

<sup>3</sup>*Department of Mechanical Engineering  
National Chiao-Tung University, Hsinchu, Taiwan*

<sup>4</sup>*Department of Mechanical Engineering  
National Taiwan University of Science and Technology  
[hocht@nfu.edu.tw](mailto:hocht@nfu.edu.tw)*

**Abstract:** In this work, we successfully developed a process to fabricate dual-channel polymeric waveguide filters based on an asymmetric Bragg coupler (ABC) using holographic interference techniques, soft lithography, and micro molding. At the cross- and self-reflection Bragg wavelengths, the transmission dips of approximately  $-16.4$  and  $-11.5$  dB relative to the 3 dB background insertion loss and the 3 dB transmission bandwidths of approximately 0.6 and 0.5 nm were obtained from an ABC-based filter. The transmission spectrum overlaps when the effective index difference between two single waveguides is less than 0.002.

© 2009 Optical Society of America

OCIS codes: (090.2880) Holographic interferometry; (220.4610) Optical fabrication; (230.1950) Diffraction gratings; (999.9999) Mold; (999.9999) Replication.

---

## References and Notes

1. T. Erdogan, "Optical add-drop multiplexer based on an asymmetric bragg coupler," *Opt. Commun.* **157**(1–6), 249–264 (1998).
2. D. Gauden, E. Goyat, C. Vaudry, P. Yvernault, and P. Pureur, "Tunable Mach-Zehnder-based add-drop multiplexer," *Electron. Lett.* **40**(21), 1374–1375 (2004).
3. M. Kulishov, V. Grubsky, J. Schwartz, X. Daxhelet, and D. V. Plant, "Tunable waveguide transmission gratings based on active gain control," *IEEE J. Quantum Electron.* **40**(12), 1715–1724 (2004).
4. M. Dainese, M. Swillo, L. Wosinski, and L. Thylen, "Directional coupler wavelength selective filter based on dispersive bragg reflection waveguide," *Opt. Commun.* **260**(2), 514–521 (2006).
5. F. Bilodeau, D. C. Johnson, S. Thériault, B. Malo, J. Albert, and K. O. Hill, "An all-fiber dense-wavelength-division multiplexer/de-multiplexer using photoimprinted Bragg grating," *IEEE Photon. Technol. Lett.* **7**(4), 388–390 (1995).
6. H. C. Tsoi, W. H. Wong, and E. Y. B. Pun, "Polymeric long-period waveguide gratings," *IEEE Photon. Technol. Lett.* **15**(5), 721–723 (2003).
7. S. Ahn, and S. Shin, "Grating-assisted co-directional coupler filter using electrooptic and passive polymer waveguides," *IEEE J. Sel. Top. Quantum Electron.* **7**(5), 819–825 (2001).
8. L. Dong, L. Reekie, and J. L. Cruz, "Long period grating formed in depressed cladding fibres," *Electron. Lett.* **33**(22), 1897–1898 (1997).
9. T. M. Butler, E. Igata, S. J. Sheard, and N. Blackie, "Integrated optical Bragg-grating-based chemical sensor on a curved input edge waveguide structure," *Opt. Lett.* **24**(8), 525–527 (1999).
10. Y. O. Noh, H. J. Lee, J. J. Ju, M. S. Kim, S. H. Oh, and M. C. Oh, "Continuously tunable compact lasers based on thermo-optic polymer waveguides with Bragg gratings," *Opt. Express* **16**, 18194–18201 (2008), <http://www.opticsexpress.org/abstract.cfm?URI=OPEX-16-22-18194>.
11. G. Jeong, J.-H. Lee, M. Y. Park, C. Y. Kim, S.-H. Cho, W. Lee, and B. W. Kim, "Over 26-nm Wavelength Tunable External Cavity Laser Based on Polymer Waveguide Platforms for WDM Access Networks," *IEEE Photon. Technol. Lett.* **18**(20), 2102–2104 (2006).
12. J. H. Lee, M. Y. Park, C. Y. Kim, S. H. Cho, W. Lee, G. J., and B. W. Kim, "Tunable External Cavity Laser Based on Polymer Waveguide Platform for WDM Access Network," *IEEE Photon. Technol. Lett.* **17**(9), 1956–1958 (2005).
13. M. C. Oh, H. J. Lee, M. H. Lee, J. H. Ahn, S. G. Han, and H. G. Kim, "Tunable wavelength filters with Bragg gratings in polymer waveguides," *Appl. Phys. Lett.* **73**(18), 2543–2545 (1998).
14. W. C. Chuang, C. T. Ho, and W. C. Wang, "Fabrication of a high resolution periodical structure using a replication process" *Opt. Express* **13**, 6685–6692 (2005), <http://www.opticsexpress.org/abstract.cfm?URI=OPEX-13-18-6685>.

15. W. C. Chuang, C. K. Chao, and C. T. Ho, "Fabrication of a high resolution periodical structure on polymer waveguide using a replication process" *Opt. Express* **15**, 8649–8659 (2007), <http://www.opticsexpress.org/abstract.cfm?URI=OPEX-15-14-8648>.
16. W. C. Chuang, C. T. Ho, and W. C. Chang, "Fabrication of polymer waveguides by a replication method," *Appl. Opt.* **45**(32), 8304–8307 (2006).
17. J. C. Lötters, W. Olthuis, P. H. Veltink, and P. Bergveld, "The mechanical properties of the rubber elastic polymer polydimethylsiloxane for sensor applications," *J. Micromech. Microeng.* **7**(3), 145–147 (1997).
18. P. Nussbaum, I. Philipoussis, A. Huser, and H. P. Herzig, "Simple technique for replication of micro-optical elements," *Opt. Eng.* **37**(6), 1804–1808 (1998).
19. M. Rossi, H. Rudmanr, B. Marty, and A. Maciossek, "Wafer-scale micro-optics replication technology," in *Lithographic and Micromaching Techniques for Optical Component Fabrication II*, E.-B. Kley and H.P. Herzig, eds., *Proc. SPIE* **5183**, 148–154 (2003).
20. M. Greenberg, and M. Orenstein, "Unidirectional complex grating assisted couplers," *Opt. Express* **12**(17), 4013–4018 (2004), <http://www.opticsexpress.org/abstract.cfm?URI=OPEX-12-17-4013>.
21. A. Yariv, *Introduction to Optical Electronics*, 3rd edition, (H. Rinehart & Winston, New York, 1984).

## 1. Introduction

Wavelength division multiplexing (WDM) has proven to be a key technology for accommodating large bandwidths for the global spread of multimedia communications in optical fiber networks. In WDM-based networks, optical add/drop multiplexer (OADM) devices used to insert (add) or extract (drop) a specific wavelength in optical fiber communication systems are essential. These components allow the extraction of a wavelength from a transmission loop and the addition of the same wavelength to the network [1]. Numerous different architectures of add/drop filters based on optical waveguides have been demonstrated. These include Mach-Zehnder interferometer (MZI) based add/drop filters [2], grating-assisted co-directional couplers [3], asymmetric Bragg coupler (ABC) based filters [1], and Bragg reflector channel waveguide filters [4]. MZI- based add/drop filters yield excellent insertion loss and channel isolation, and they can be built on both all-fiber and integrated-optics platforms. However, their performance is extremely sensitive to the balance of the interferometer and relative placement of the two gratings; therefore, some post-fabrication trimming is often necessary [5]. A grating-assisted co-directional coupler, consisting of two dissimilar waveguides and a long period grating, has been widely discussed for use as a wavelength filter. It has the advantage of a long grating period (about a few tens of micrometers), facilitates the fabrication by using standard photolithography, and has a low back-reflection characteristic, avoiding unwanted optical resonances [6]. The main drawback of such a device is that when it operates in a small spectral bandwidth, a long interaction grating length (about a few hundreds of grating periods) is required [7]; therefore, it is not beneficial for device integration. Bragg reflector channel waveguide filters have excellent return loss and crosstalk characteristics and are inherently very stable. However, the need for non-reciprocal optical circulators limits its application in integrated optical formats. ABC-based filters, which operate in a contra-directional mode, are not sensitive to grating placement for obtaining a desired filter spectrum. Therefore, they have better stability and reproducible mass production than MZI-based filters.

Polymeric materials offer a conceivable platform to fabricate complex yet affordable integrated optical devices, especially dense wavelength division multiplexers, on a planar substrate; this is due to the benefits of low production cost, easy processing, and mechanical flexibility. Polymer surface-relief Bragg grating, which provides a narrow bandwidth, low crosstalk, and flat-top pass band, has become an essential component for various applications in optical communications and optical sensing [8]. For example, Butler et al used polymer surface-relief Bragg grating on an integrated optical waveguide structure to fabricate a chemical sensor [9]. Noh et al demonstrated a cost-effective tunable wavelength laser based on the thermo-optic tuning of a polymer waveguide Bragg reflector for WDM optical communications [10]. Other applications of tunable lasers and filters were demonstrated in Ref [11–13].

We recently demonstrated a process to rapidly produce submicron range gratings on a waveguide for optical filters using soft lithography, micro-molding, and holographic interference techniques. In this method, the grating structure on a polymer is first fabricated

using holographic interferometry and the micro-molding processes. Polymeric wavelength filters are produced by a two-step molding process where the master mold is first formed on a negative tone photoresist and subsequently transferred to a PDMS mold; following this step, the PDMS silicon rubber mold is used as a stamp to transfer the pattern of the polymeric wavelength filters onto a UV cure epoxy. A high aspect ratio and vertical waveguide sidewalls are obtained by this method, and consistent reproduction of the grating on a UV polymer has been achieved with this process [14,15]. In this paper, we describe a technique that combines the holographic interferometry, soft lithography, and a simple replication processes for fabricating a polymeric ABC.

Polymeric ABC filters were constructed using the planar channel waveguide configuration. A pair of parallel channel waveguides with different widths was embedded into a planar substrate (Fig. 1). The two waveguides are asynchronous because the effective refractive indices of the two waveguides are quite different. In spite of the large index mismatch between the two waveguides, an efficient power coupling was achieved using the Bragg grating engraved on the bottom of the two waveguides. The maximum cross-reflection power coupling occurred at a specific wavelength  $\lambda_{d1}$  (Bragg wavelength) satisfying the Bragg reflection condition,  $(n_{eff1} + n_{eff2}) \Lambda = \lambda_{d1}$ , where  $n_{eff1}$  and  $n_{eff2}$  are the effective indices of the two waveguide modes and  $\Lambda$  is the grating period. It implies that the center wavelength of the ABC filter is proportional to the sum of the effective indices of the two individual waveguides. Therefore, when the effective index of any individual waveguide was changed it results in a shift in the center wavelength. Furthermore, an unwanted reflection wavelength, denoted by self-reflection Bragg wavelength ( $\lambda_{d2}$ ), caused by the grating of input waveguide is occurred in the input end. The self-reflection light results in broadening the transmission spectrum of the filters, if its spectrum overlaps with the spectrum of cross-reflection light. Such unwanted reflection light can be eliminated by suppressing the grating depth of the input waveguide. Another method is to make the two decoupled waveguides quite dissimilar to avoid the spectrum overlapping.

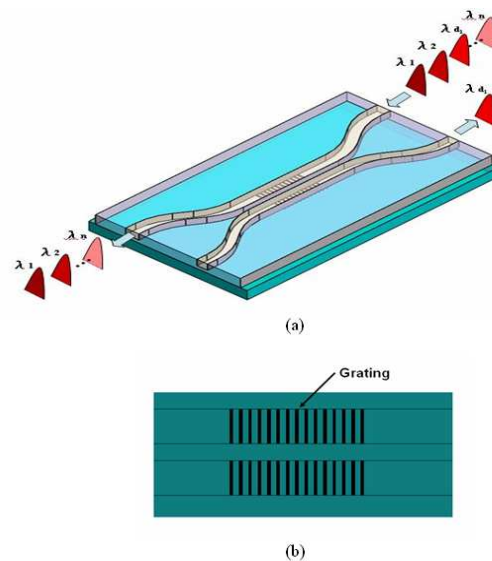


Fig. 1. (a) Schematic diagram of a polymeric asymmetric Bragg coupler (ABC) (b) The Close-up view of the coupling/grating region directly from above

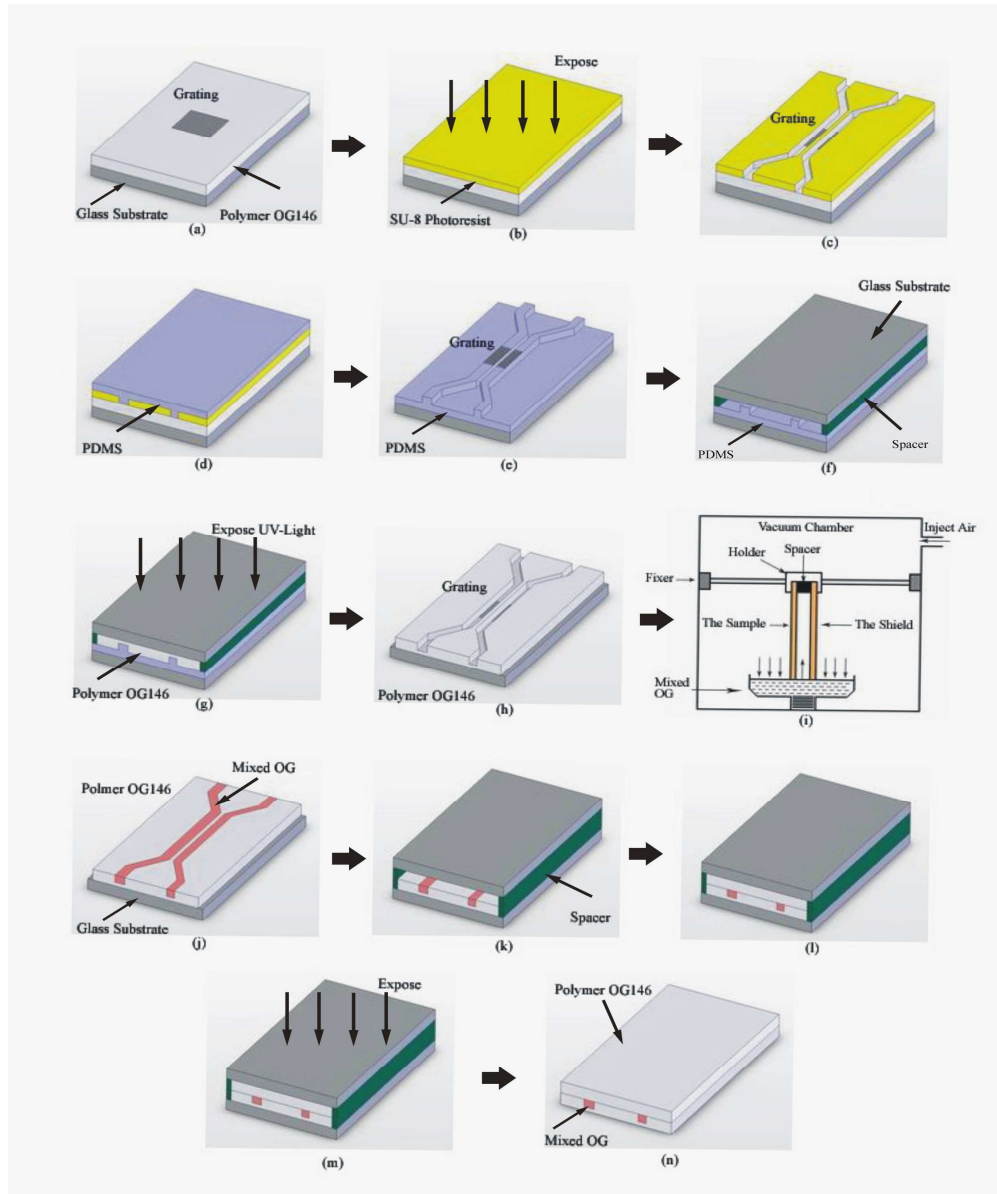


Fig. 2. Fabrication process of buried gratings in polymeric waveguide filter structures: (a) UV polymer with gratings is deposited on the glass (b) The photoresist is exposed to UV light (c) The photoresist mold (d) PDMS is poured into the photoresist mold (e)The PDMS mold (f) A spacer with a thickness of  $400\mu\text{m}$  is positioned (g) An OG146 pre-cured epoxy is injected into the space (h) A hardened epoxy forms the cladding layer of the ABC filter (i) A rectangular channel is formed (j) A mixed OG epoxy is injected into the channel (k)The epoxy in the channel is then cured by exposure to UV light, and the cover glass and the PDMS layer are removed from the sample (l) A spacer with a thickness of  $410\mu\text{m}$  is positioned (m) The OG146 epoxy is injected into the channel (n) The final polymeric ABC filter.

## 2. Grating Fabrication

A three-step process for the rapid prototyping of grating structures on a polymer substrate involving was carried out first. A grating pattern was holographically exposed using a two-beam interference pattern on a positive photoresist film (Ultra 123, MicroChem Corp., MA.;

refractive index = 1.618). This produced a master that was subsequently used to produce a polydimethylsiloxane (PDMS) mold. This silicone rubber mold was then used as a stamp to transfer the gratings pattern onto a UV cure epoxy polymer (OG146, Epoxy Technology Inc., USA). The refractive index of epoxy polymer is increased by about 0.03 after curing. The refractive index of cure epoxy polymer is about 1.5201 at 1550nm, which was measured by using prism coupler system (Model 2010, Metricon Inc., USA). The details of the process involved in grating fabrication are described in our previous reports [14]. The UV polymer with grating was cut down to dimensions of 1cm  $\times$  5cm, and the dimensions of the gratings on the polymer were 0.9 cm long and 1 mm wide.

### 3. Fabrication of the asymmetric Bragg couplers (ABC)

In order to fabricate asymmetric Bragg couplers (ABC), a 700- $\mu$ m thick glass substrate was first cut into a 5cm  $\times$  1cm rectangle. After substrate cleaning, the UV polymer (OG146 with a grating period of 510nm and grating depth of 350nm was deposited on the glass [14]; it was coated with a 7.0  $\mu$ m thick negative photoresist (SU-8) spun on at 1000 rpm for 17 seconds. Samples were exposed through polyethylene terephthalate (PET)-based masks using a UV mask aligner (AB-Manufacturing, CA) for 90 seconds; this was followed by development in a SU-8 developer (MicroChem) for 45 seconds to obtain a negative waveguide pattern with gratings on the bottom. The process flow is shown in Figs. 2 (a) - (c). In this study, several configurations of ABC filters are fabricated for optical characteristic comparison. The details of the process are described in the previous reports [16].

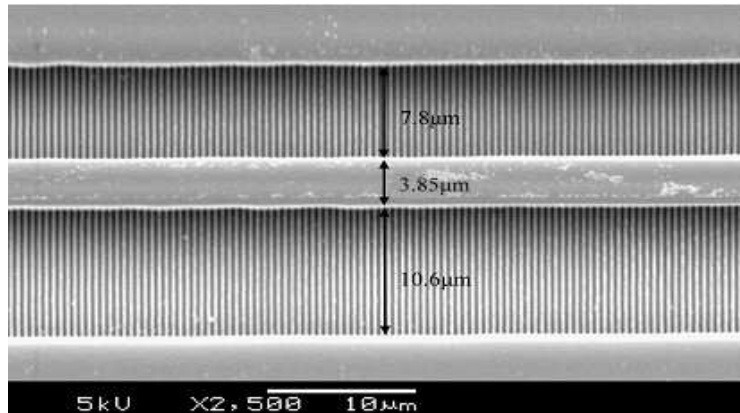


Fig. 3. SEM micrograph of the waveguide pattern on the photoresist, which showed an intact grating pattern inside the groove; the SEM was tilted 4° degree (dimensions are 7.8  $\mu$ m  $\times$  7  $\mu$ m and 10.6  $\mu$ m  $\times$  7  $\mu$ m, the length is 5 cm, the gap is about 3.85  $\mu$ m, and the grating period is 510nm).

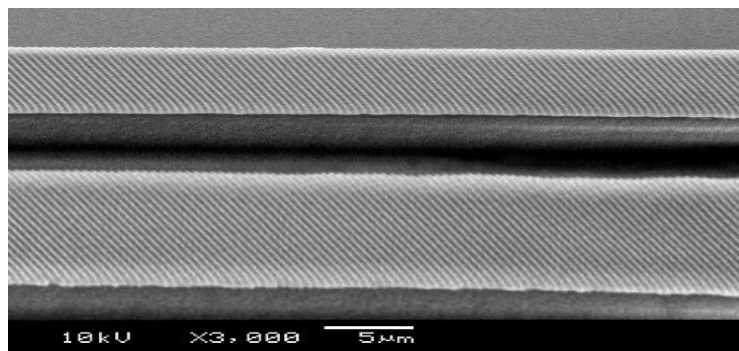
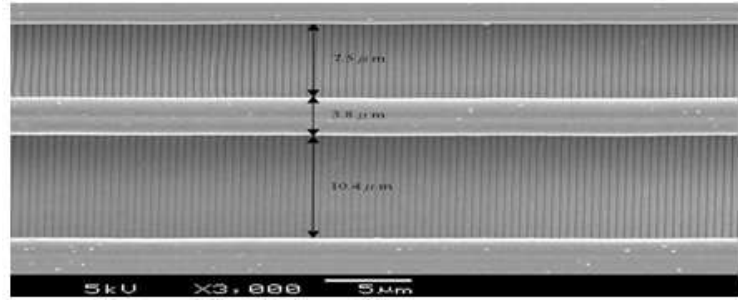
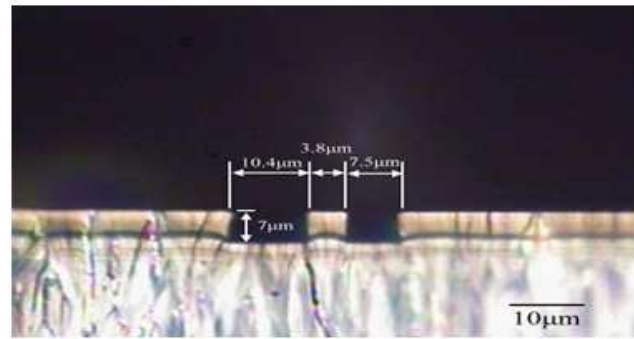


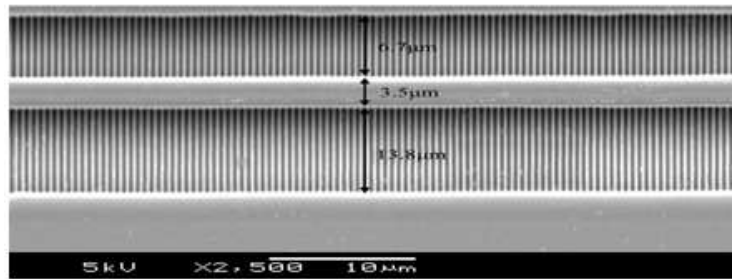
Fig. 4. SEM micrograph of the PDMS waveguide with gratings; the SEM was tilted 25° (the grating period is 510nm, and the grating depth is 350nm).



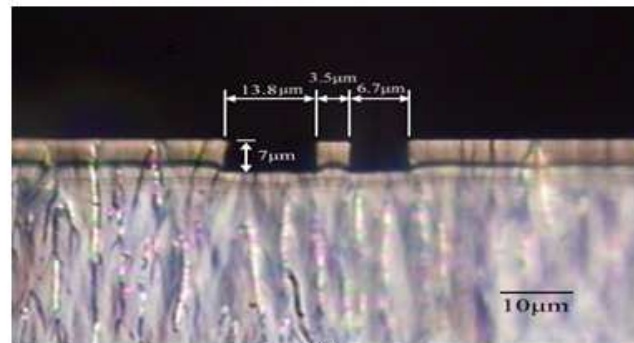
(a)



(b)



(c)



(d)

Fig. 5. SEM and optical micrograph of the OG146 rectangular groove showing the intact grating pattern inside the groove; the SEM was tilted  $5^\circ$  degree (a) SEM of sample 1 (b) OM of sample 1 (c) SEM of sample 2 (d) OM of sample 2. (for Figs. 5(a) and 5(c), dimensions are  $7.5\mu\text{m} \times 7\mu\text{m}$  and  $10.4\mu\text{m} \times 7\mu\text{m}$ , the length is 5cm, the gap is about  $3.8\mu\text{m}$ , and the grating period is 510nm. For Figs. 5(b) and 5(d), dimensions are  $6.7\mu\text{m} \times 7\mu\text{m}$  and  $13.8\mu\text{m} \times 7\mu\text{m}$ , the length is 5cm, the gap is about  $3.5\mu\text{m}$ , and the grating period is 510nm.).

An SEM image of the first waveguide mold was taken after the photoresist mold was fabricated (Fig. 3), showing the intact grating pattern inside the groove. The patterned resist was used as a mother mold to transfer the pattern onto a polydimethylsiloxane (PDMS) thin film using typical micro-molding techniques (e.g., stamping) [17–19]. The diluted PDMS was coated uniformly onto the patterned photoresist. After baking at 90°C for 1 hr, the PDMS was cured and was easily peeled off from the photoresist (Figs. 2(d)-(e)). Fig. 4 shows the SEM image of the PDMS waveguide with gratings. The waveguide with the gratings pattern was transferred onto a UV polymer (OG146) from the PDMS mold using the UV replication process described by Rossi and our previous reports (Figs. 2(f)-(h)) [14,19]. A spacer with a thickness of 400 $\mu\text{m}$  was placed between the mold and a thin Pyrex glass slide. After injecting the precured UV polymer (OG146), the epoxy was then cured under a broadband UV light operating in a wavelength range of 300–400nm. After the polymer was completely cured, it was easily peeled off from the mold. The SEM images show that the replication on epoxy was good (Figs. 5 (a) and (c)), and matched the negative photoresist mold dimension well. The optical microscope (OM) images show the end faces of the cross-section of the two ABC filters (Figs. 5 (b) and (d)). After separation from the PDMS mold, a hardened epoxy with gratings formed the cladding layer of the polymer waveguide filter. For Sample 1, the dimensions of waveguide grooves are 7.5  $\mu\text{m}$   $\times$  7  $\mu\text{m}$  and 10.4  $\mu\text{m}$   $\times$  7  $\mu\text{m}$ , the length is 5 cm, and the gap is approximately 3.8 $\mu\text{m}$ ; for Sample 2, the dimensions are 6.7  $\mu\text{m}$   $\times$  7  $\mu\text{m}$  and 13.8  $\mu\text{m}$   $\times$  7  $\mu\text{m}$ , the length is 5 cm, and the gap is approximately 3.5 $\mu\text{m}$ .

To form the waveguide core, a similar UV epoxy (mixed OG) was injected into the groove. Instead of the spin-coating technique, which could create a thick unguided layer outside the core region resulting in some coupling loss during the input of the optical fiber to the filter, another method was proposed (Figs. 2(i)-(j)). A thin layer of a polydimethylsiloxane (PDMS) polymer was spun onto a glass slide that was then placed over the epoxy groove, forming a rectangular tunnel.

In order to inject the high-viscosity epoxy of OG154 into the rectangular channel, we diluted OG154 with another UV epoxy OG169 (mixing ratio of 1:1) to reduce the viscosity. After the curing process, the refractive index of the mixed epoxy was approximately 1.555 at 1550nm. Then, a drop of the mixed UV epoxy was injected into the channel from one of the open ends. After exposure to UV light, the epoxy end of the tunnel was sealed. Next, the sample was inserted into the liquid epoxy with the open-end face down. This process was carried out in a vacuum chamber (Fig. 2(i)). When the pressure in the chamber reached  $10^{-3}$  torr, air was introduced into the chamber to force the liquid epoxy into the tunnel. The epoxy in the tunnel was cured by exposure to UV light for 1–2 min. After the cover glass was removed, the PDMS layer was peeled off from the sample. To prevent optical loss due to either surface scattering losses or the outright absence of a guided mode for the asymmetric waveguide structure, the upper cladding layer was used. The same UV epoxy (OG146) was deposited using the fabricating procedure described in the previous section (Figs. 2(k)-(n)). A spacer with a thickness of 410 $\mu\text{m}$  was placed between the sample and a thin Pyrex glass slide. After injecting the precured UV polymer (OG146) into the opening between the mold and the glass slide, UV light was used to crosslink the polymer. The sample was diced and the end-faces were polished; the final polymeric ABC filter was 4cm in length, 1cm in width and approximately 810 $\mu\text{m}$  in thickness (Fig. 2(n)).

#### 4. Simulation

The waveguide properties, including the mode pattern and the effective index, were simulated using the beam propagation method (BPM\_CAD, Opti-Wave Inc., Canada). In order to prevent co-directional evanescent coupling to obtain excellent crosstalk performance, we used highly asymmetric waveguides for the coupler to have compound modes confined to each single waveguide [20]. In our case, the compound modes provided good approximations for the modes of single waveguides. Figs. 6 (a) and (b) show the fundamental modes of the single waveguides, and Figs. 6(c) and (d) show the compound modes of the ABC coupler in Sample 2.



The effective indices of the compound modes for Sample 2 are  $n_{eff1} = 1.55149$  and  $n_{eff2} = 1.54964$  (Table 1), corresponding to the single waveguide modes  $n_{eff1.s} = 1.55155$  and  $n_{eff2.s} = 1.54958$ , respectively. The overlap integrals between the single and the compound modes are 98.25% and 97.95% for the first and second modes, respectively. The simulation result shows the waveguides in the sample are highly asymmetry. The effective indices for the single waveguides of Sample 1 are 1.55101 and 1.55005, as obtained from the simulation (Table 1).

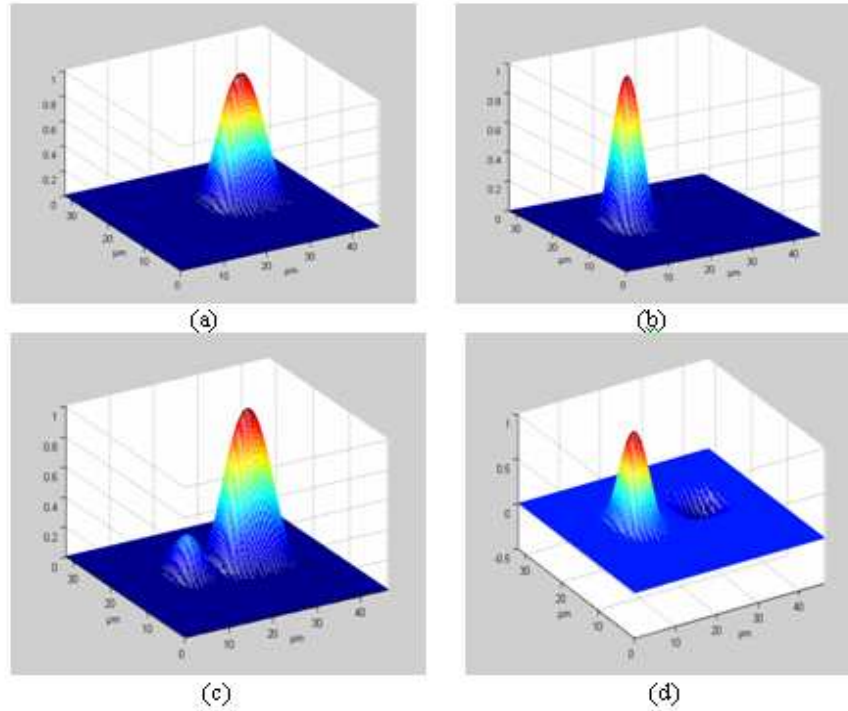


Fig. 6. (a) Fundamental mode of the single waveguide; width  $w = 13.8\mu\text{m}$  (b) Fundamental mode of the single waveguide; width  $w = 6.7\mu\text{m}$  (c) and (d) The first compound mode of the coupler structure in (d) The second compound modes of the coupler. (Sample 2).

The cross-reflection Bragg wavelengths  $\lambda_{d1}$  are 1581.5406 and 1581.5763 nm and the self-reflection Bragg wavelengths  $\lambda_{d2}$  ( $\lambda_{d2} = 2 n_{eff2} \Lambda$ ) are 1581.041 and 1580.5716 nm (Table 1), as calculated from the Bragg reflection conditions for the Sample 1 and 2 filters, respectively, with a grating period of 510nm. When the core refractive index ranges from 1.549 to 1.560 for a mixing ratio of OG154 of 45-60 vol.%, the calculated cross-reflection Bragg wavelength through the beam propagation method varies from 1575.5578 to 1586.5498 nm for Sample 1 and from 1575.5945 to 1586.5822 nm for Sample 2. Using the simulation, the transmission of the optical filter can be calculated using the coupled mode theory [21], and the calculated results were shown in Fig. 10 and Table 1.



**Table 1. The simulation and measurement results of sample 1 and sample 2**

	The simulation results				The measurement results			
	The effective index		Bragg wavelength ( $\mu\text{m}$ )		Bragg wavelength ( $\mu\text{m}$ )		The transmission dips at Bragg wavelength (dB)	
	$n_{\text{eff}1}$	$n_{\text{eff}2}$	Cross-reflection	Self-reflection	Cross-reflection	Self-reflection	Cross-reflection	Self-reflection
Sample 1	1.55101	1.55005	1581.5406	1581.041	1581.6	1581	-12.1	-16.3
Sample 2	1.55155	1.54958	1581.5763	1580.5716	1581.3	1580.3	-11.5	-16.4

### 5. Measurement

The near-field patterns of the optical waveguide were observed using the end-fire coupling technique. Fig. 7 shows the schematic diagram of the measurement system. An amplified spontaneous emission (ASE) source with a wavelength range of 1530-1560 nm was used as the wideband light source (Stabilized Light Source, PTS-BBS, Newport Inc., USA). The light source was polarized in the TE direction using the in-line polarizer (ILP-55-N, Advanced Fiber Resources, China), which was followed by a polarization controller with an operation wavelength of around 1550nm (F-POL-PC, Newport Inc., USA). The polarization state is examined by using near infrared precision linear polarizer (20LP-NIR, Newport Inc., USA). The output mode field of the waveguide was observed using an IR-CCD system (Model 7290A, Micron Viewer, Electrophysics Inc., USA) with image analysis software (LBA-710PC-D, V4.17, Spiricon Inc., USA) to show the single-mode characteristics of the waveguide. Fig. 8 shows the field intensity distribution of the two-waveguide-coupled region for Sample 2; the ASE laser light was shone onto the narrow waveguide end; the high asymmetric mode profile can be observed as well.

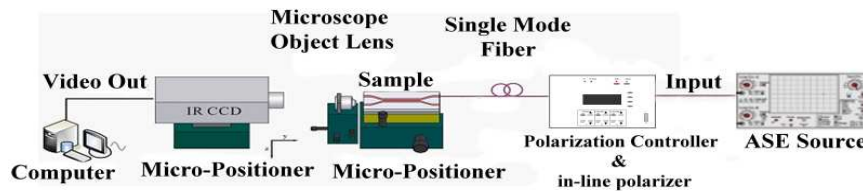


Fig. 7. Schematic diagram of the mode field measurement system

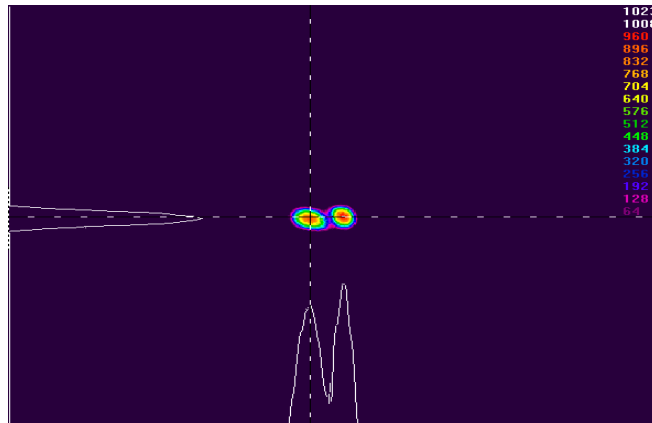


Fig. 8. Near-field pattern for the ABC filter of Sample 2.

The spectral characteristics of the ABC-based filter were measured using a tunable laser system (Q8384 Optical Spectrum Analyzer, Advantest Inc., Japan). The output fiber of the tunable laser is of Panda-type polarization maintaining fiber, with TE mode in the slow axis in line with vertical direction. Again, a tunable laser light source with a wavelength range of 1511-1620 nm was used as the wideband light source and followed by a polarization controller. An alignment He-Ne laser source, used as the auxiliary source, was combined with the wideband source using a  $2 \times 1$  optical fiber coupler. The optical filter was set on a micro-positioner, and two single mode fibers were used as the input and output fibers. The input light source was polarized in the TE direction, as was the mode field measurement system. The output fiber was then connected to the receiver end of the tunable laser to characterize the filter performance. The measurement schematic diagram is depicted in Fig. 9. The tunable laser was coupled onto the narrow waveguide ends of the filters and coupled out from the alternative end of the same waveguides. The measured results which are similar to the theoretical results depicted in Figure.10. Apart from for the upper transmission dips, which resulted from the cross-reflection Bragg condition ( $\lambda_{d1}$ ), a lower transmission dip resulting from the self-reflection Bragg condition ( $\lambda_{d2}$ ) was observed as well.

At the cross-reflection Bragg wavelength, a transmission dips of  $-12.1$  and  $-11.5$  dB were obtained for Samples 1 and 2, respectively (Table 1). At the self-reflection Bragg wavelength, the dips were  $-16.3$  and  $-16.4$  dB for Samples 1 and 2 (Table 1), respectively. The measured cross-reflection Bragg wavelengths were 1581.6 and 1581.3nm, which are off approximately 0.06 and 0.28nm from the theoretical predictions for Samples 1 and 2, respectively. The measured self-reflection Bragg wavelengths were 1581.0 and 1580.3nm, which are off approximately 0.04 and 0.27nm from the theoretical predictions for Samples 1 and 2, respectively. The 3dB transmission bandwidth of Sample 2 is approximately 0.5 and 0.6nm for the cross-reflection and self-reflection modes, respectively. Nevertheless, for Sample 1, the transmission spectra for cross- and self-reflection overlap due to small differences between the effective indices of the two single waveguides. Different samples with the difference of the effective index between two waveguides have been used, and the transmission spectra of cross- and self-reflection would overlap when the difference is below 0.002. The results of Sample 2 show that the effective index difference should be greater than 0.002 to prevent spectrum overlapping.

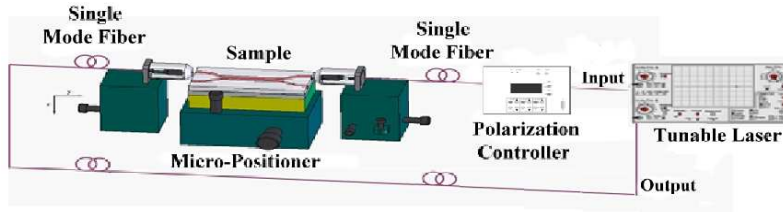


Fig. 9. . Optical setup for transmission spectrum measurement.

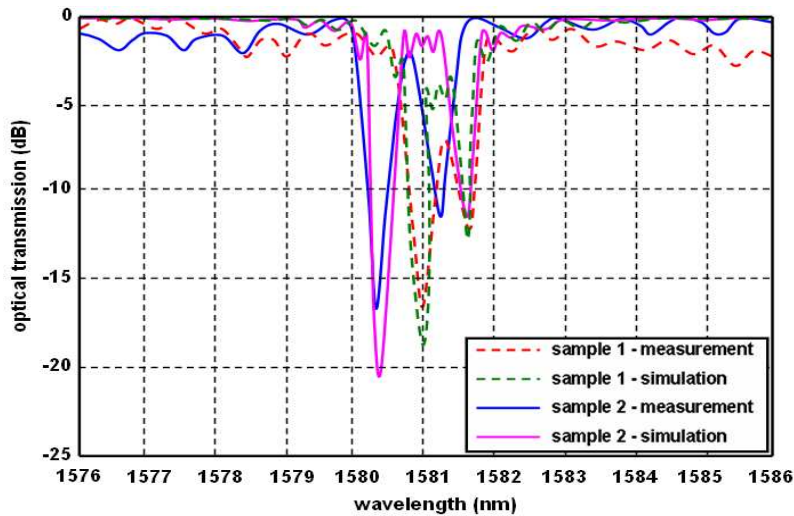


Fig. 10. Transmission spectra of an ABC filter with a 0.9cm-long grating length.

## 6. Conclusion

We successfully developed a process to fabricate dual-channel polymeric waveguide filters based on an asymmetric Bragg coupler. In this work, the grating structure on a polymer is fabricated first using holographic interferometry and micro-molding processes. The ABC filters are produced by a two-step molding process where the master mold is first formed on a negative tone photoresist and subsequently transferred to a PDMS mold; following this step, the PDMS silicon rubber mold was used as a stamp to transfer the pattern of the ABC filters onto a UV cure epoxy. For an ABC filter with dimensions of  $6.7\mu\text{m} \times 7\mu\text{m}$  and  $13.8\mu\text{m} \times 7\mu\text{m}$ , length of 5cm, gap of  $3.5\mu\text{m}$ , grating length of 0.9cm, grating period of 510nm, and grating depth of 350nm, the transmission dips are approximately  $-16.4$  and  $-11.5$ dB, and the 3dB transmission bandwidths are approximately 0.6 and 0.5nm. The transmission spectrum overlaps when the effective index difference between two single waveguides is less than 0.002. This process shows great potential for mass production of any grating structure on polymer waveguides.